JCTC Journal of Chemical Theory and Computation

ARTICLE

pubs.acs.org/JCTC

Free Energy Landscapes of Alanine Dipeptide in Explicit Water Reproduced by the Force-Switching Wolf Method

Yasushige Yonezawa,*,† Ikuo Fukuda,‡ Narutoshi Kamiya,† Hiromitsu Shimoyama,† and Haruki Nakamura†

†Institute for Protein Research, Osaka University, 3-2 Yamadaoka, Suita, Osaka 565-0871, Japan

‡Computational Science Research Program, RIKEN, 2-1, Hirosawa, Wako, Saitama 351-0198, Japan

ABSTRACT: Precise and rapid calculation of long-range interactions is of crucial importance for molecular dynamics (MD) and Monte Carlo simulations. Instead of the Ewald method or its high speed variant, PME, we applied our novel method, called the force-switching Wolf method, to computation of the free energy landscapes of a short peptide in explicit water. Wolf and co-workers showed that long-range electrostatic energy under a periodic boundary condition can be well reproduced even by truncating the contribution from the distant charges, when the charge neutrality is taken into account. We recently applied the procedure proposed by Wolf and co-workers to a mathematically consistent MD theory by means of a force-switching scheme, and we show that the total electrostatic energy for sodium chloride liquid was well conserved and stable during the MD simulation with the force-switching Wolf method. Our current results for an aqueous peptide solution with a series of canonical and multicanonical molecular dynamics simulations show that the force-switching Wolf method is not only in good accordance with the energies and forces calculated by the conventional PME method but also properly reproduces the solvation and the free energy landscapes of the peptide at 300 K.

INTRODUCTION

Molecular dynamics (MD) and Monte Carlo (MC) simulations are now indispensable and widely used for studies of condensed matter, such as nano- and biomolecular systems. In these simulations, most of the computational time is usually consumed by calculations of nonbonded long-range, electrostatic interactions. The long-range interactions determine thermodynamic, structural, and dynamical properties of the systems. Therefore, fast and accurate methods for computing the interactions are required for reliable MD and MC applications.

There are various algorithms proposed for computing the long-range electrostatic interactions. Truncation of interactions (the cutoff method) was formerly the most widely used, but it introduces serious errors and artifacts in the treatment of the energies and forces.[1] The reaction field method,[2] cell-multipole method,[3] fast-multipole method,[4] and smooth-cutoff potential method[5] have been developed to overcome these problems.

The Particle Mesh Ewald (PME) method,[6,7] a computationally efficient alternative to the Ewald method, takes advantage of the Fast Fourier Transform algorithm and is now widely accepted as the standard to calculate electrostatic interactions among charged particles of molecular systems under periodic boundary conditions. However, the Ewald method has intrinsic artifacts, as pointed out by many researchers.[8−10] Moreover, because of network communication problems of the Fast Fourier Transfer algorithm employed in the PME method, it is hard to accomplish good scalability with respect to large systems in highly parallel computations.[11,12]

Wolf et al. proposed an algorithm, in which charge neutrality and potential damping are applied to the cutoff method, and it achieves fairly good accuracy, comparable to the Ewald method, for simulations of NaCl and MgO in crystalline and liquid phases.[13] The algorithm, hereafter referred to as the Wolf method, is easy to parallelize and is computationally very efficient like the original cutoff method, because no reciprocal space calculations are necessary. In the past decade, the Wolf method attracted a great deal of attention and has been evaluated in many applications. Demontis et al. used this method in simulation studies of liquid water and in anhydrous and hydrated aluminosilicates. They showed that the method is computationally more efficient than the PME method when the damping parameter is carefully chosen.[14] Zahn et al. proposed a modification of the Wolf method to apply it to molecular liquids in MD simulations and obtained results comparable to those of the PME method in the TIP3P and SPC water systems.[15] Ma and Garofalini applied the Wolf method to β-SiC crystals with a short-range correction in MD and obtained results that were very close to experimental data.[16] Avendaño and Gil-Villegas used the Wolf method in MC to simulate properties of electrolyte solutions and molten salts and showed that the Wolf method reproduced the simulation data produced using the PME method.[17] Fennell and Gezelter proposed another modification to the original Wolf method, referred to as the Fennell method hereafter.[18] This method was also shown to reproduce the results of MD simulations of NaCl crystals using the PME method.

Kikugawa et al. applied the Fennell method both to globular proteins in explicit water and to membrane proteins immersed in lipid bilayers with explicit water.[19] They obtained results comparable to the PME method with respect to not only the energies and forces but also the dynamics of the radial distribution function for the solvent and conformational dynamics of the proteins. Moreover, they demonstrated that the Fennell method realizes fast MD calculations using the special purpose MD engine MDGrape-3 and is highly scalable in parallel on a PC cluster connected by high speed networks.

Received: June 28, 2010
Published: March 30, 2011

Recently, Fukuda et al. pointed out that there is an inconsistency between forces and energies in the formulation of the Wolf method. They then proposed an improved method, in which the inconsistency is completely removed using the force-switching scheme.[20] Hereafter, we call it the force-switching Wolf (FSw-Wolf) method. They confirmed that the electrostatic energy of the FSw-Wolf method for the sodium and chloride liquid system is comparable to that of the Ewald method and that it produces more exact energy conservation properties than those of the original Wolf method.

In this report, in order to investigate the applicability of the FSw-Wolf method to biological molecular systems, we evaluated the method for an alanine-dimer peptide in explicit water under periodic boundary conditions. We here focus our attention just on a comparison between the FSw-Wolf method and the PME method. This system would not produce any significant artifacts, due to the periodicity applied in the PME, if the configuration sampling is completed. In fact, in studies of similar systems, Villarreal and Montrich recently reported that incomplete sampling of explicit solvent of solvated biomolecular systems is likely to affect the results to a greater extent compared to the artifact induced by the Ewald method.[21] To effectively utilize the sampling data, the free energy is a good measure, since it is strongly affected by the quality of the sampling data, especially in biological systems. Consequently, we show that when the parameters are sufficiently optimized, the energies, forces, and radial distribution functions of the FSw-Wolf method are comparable to the PME method in canonical molecular dynamics simulations. Moreover, we show that the dipole−dipole interactions of water molecules calculated by the FSw-Wolf method are similar to those obtained by the PME method. In order to precisely evaluate the free energy landscape using the FSw-Wolf method, we carried out multicanonical molecular dynamics (McMD) simulations[22−27] for the peptide system, and we compared the results from the PME method with those from the FSw-Wolf method. The McMD simulation is one of the generalized-ensemble methods, and it allows us to investigate the free energy landscape involving rare events separated by the large barriers, which are not attained by canonical MD simulations. Such a reliable estimation of the free energy using the McMD simulation with the Wolf type method has not been ever performed for biomolecular systems.

MATERIAL AND METHODS

Wolf Method. The Wolf method has been described elsewhere.[13] We briefly introduce the algorithm. The electrostatic potential has a long-range nature as it slowly decreases as the inverse of the distance between the charged particles. The effective range is thought to be infinite. Therefore, some particular treatment is required for the integration of an infinite charge distribution. The form of the pure electrostatic potential E_{coloumb} is

$$E_{\mathrm{coulomb}} = \frac{1}{2}\sum_{i=1}^{N}\sum_{j(\neq i)}^{N}\frac{q_i q_j}{|\mathbf{r}_{ij}|} \tag{1}$$

where the summation runs over all charged particles. q_i stands for the charge of the ith atom and $|r_{ij}|$ the distance between the ith and jth atoms.

The cutoff method calculates only interactions between the particles within radius R_c of each other, which creates an artificially charged sphere. This introduces large inaccuracies as indicated by Wolf et al.[13] They proposed a way to eliminate this artifact by introducing a charge neutrality condition within the cutoff sphere and potential damping using the erfc. The total electrostatic energy E_{wolf} can be written as

$$E_{\mathrm{wolf}} = \sum_{i=1}^{N}\sum_{\substack{j(>i)\\ |\mathbf{r}_{ij}|<R_C}}\left[\frac{q_i q_j \mathrm{erfc}(\alpha|\mathbf{r}_{ij}|)}{|\mathbf{r}_{ij}|} - \lim_{|\mathbf{r}_{ij}|\to R_c}\left\{\frac{q_i q_j \mathrm{erfc}(\alpha|\mathbf{r}_{ij}|)}{|\mathbf{r}_{ij}|}\right\}\right] - \left(\frac{\mathrm{erfc}(\alpha R_c)}{2R_c} + \frac{\alpha}{\sqrt{\pi}}\right)\sum_{i=1}^{N} q_i^2 \tag{2}$$

where R_c is the cutoff distance, α represents a damping parameter that determines the speed of the convergence of the summation, and N is the number of atoms. The second term on the right-hand of eq 2 is a representation of the charge neutrality regarding the atoms in the cutoff sphere other than the center atom i. The third term represents the contribution by atom i; the last is the self-energy. Using this approach, it is possible to precisely reproduce the Madelung energy.

THE FORCE-SWITCHING WOLF METHOD

Fukuda et al.[20] have pointed out that the negative derivative of the Wolf potential energy is not consistent with the force of the Wolf method, which was proposed in the original paper by Wolf et al.[13] This inconsistency should be a source of serious systematic error when applied to molecular dynamics simulations. Fukuda et al. then modified the Wolf method to fulfill the consistency using the force-switching scheme, and they demonstrated that the FSw-Wolf method satisfied energy conservation much better than the original Wolf method.

The total energy $E_{\mathrm{FSw\text{-}Wolf}}$ of the FSw-Wolf method is presented by the following equations,

$$E_{\mathrm{FSw\text{-}Wolf}} = \frac{1}{2}\sum_{i=1}^{N}\sum_{j(\neq i)} q_i q_j \tilde{V}(|\mathbf{r}_{ij}|) - \left[\frac{\mathrm{erfc}(\alpha r_1)}{2r_1} - \frac{V^*(r_1)}{2} + \frac{\alpha}{\sqrt{\pi}}\right]\sum_i q_i^2 \tag{1.1}$$

where

$$\tilde{V}(|\mathbf{r}_{ij}|) \equiv \begin{cases} \dfrac{\mathrm{erfc}(\alpha|\mathbf{r}_{ij}|)}{|\mathbf{r}_{ij}|} + V^*(r_1) - \mathrm{erfc}(\alpha r_1)/r_1 & \text{for } 0 < |\mathbf{r}_{ij}| < r \\ V^*(|\mathbf{r}_{ij}|) & \text{for } r_1 \le |\mathbf{r}_{ij}| \le r_c \\ 0 & \text{for } r_c < |\mathbf{r}_{ij}| < \infty \end{cases} \tag{1.2}$$

Here, r_1 and r_c stand for the switching length (described below) and the cutoff length, respectively. In the current study, according to a report by Fukuda et al.,[20] we employed $r_c - r_1 = 1$ Å. V^* is determined so that the force smoothness is satisfied in the entire range by the force-switching scheme as follows:

$$\mathbf{f}^i_{\mathrm{FSw-Wolf}} = \sum_{j(\neq i)} q_i q_j \tilde{F}(|\mathbf{r}_{ij}|)\frac{\mathbf{r}_{ij}}{|\mathbf{r}_{ij}|} \tag{1.3}$$

where

$$\tilde{F}(|\mathbf{r}_{ij}|) = \begin{cases} F(|\mathbf{r}_{ij}|) & \text{for } 0 < |\mathbf{r}_{ij}| < r_1 \\ F^*(|\mathbf{r}_{ij}|) & \text{for } r_1 \le |\mathbf{r}_{ij}| \le r_c \\ 0 & \text{for } r_c < |\mathbf{r}_{ij}| < \infty \end{cases} \tag{1.4}$$

and

$$F(|\mathbf{r}_{ij}|) \equiv \frac{\mathrm{erfc}(\alpha|\mathbf{r}_{ij}|)}{|\mathbf{r}_{ij}|^2} + \frac{2\alpha}{\sqrt{\pi}} \frac{\exp(-\alpha^2|\mathbf{r}_{ij}|^2)}{|\mathbf{r}_{ij}|} \tag{1.5}$$

Here, we set $F^*(|\mathbf{r}_{ij}|)$ to have the following fourth polynomial equation form:[28]

$$F^*(|\mathbf{r}_{ij}|) \equiv \alpha' + \beta|\mathbf{r}_{ij}| + \gamma|\mathbf{r}_{ij}|^2 + \delta|\mathbf{r}_{ij}|^3 \tag{1.6}$$

Thereby, we obtained the values of the coefficients satisfying the smoothness condition at r_1 and r_c as

$$\begin{bmatrix} \alpha' \\ \beta \\ \gamma \\ \delta \end{bmatrix} = \frac{1}{(r_c - r_1)^3} \begin{bmatrix} (-r_c r_1 b + r_c a + r_1^2 b - 3a r_1) r_c^2 \\ (b r_c^2 + r_c r_1 b - 2 r_1^2 b + 6 a r_1) r_c \\ -(2 b r_c^2 - r_c r_1 b + 3 r_c a - r_1^2 b + 3 a r_1) \\ b r_c - b r_1 + 2a \end{bmatrix} \tag{1.7}$$

with $a = F(r_1)$ and $b = \mathrm{d}F(r_1)/\mathrm{d}r$.

Thus, $V^*(|\mathbf{r}_{ij}|)$ is expressed as the following:

$$V^*(|\mathbf{r}_{ij}|) = -\left(\alpha'|\mathbf{r}_{ij}| + \frac{\beta|\mathbf{r}_{ij}|^2}{2} + \frac{\gamma|\mathbf{r}_{ij}|^3}{3} + \frac{\delta|\mathbf{r}_{ij}|^4}{4}\right) + \left(\alpha' r_c + \frac{\beta r_c^2}{2} + \frac{\gamma r_c^3}{3} + \frac{\delta r_c^4}{4}\right) \tag{1.8}$$

In the Appendix, we describe the details of implementation of the FSw-Wolf method for biomolecular system with the potential energies associated with the covalent bonds.

Canonical Molecular Dynamics Simulations. We employed alanine-dimer peptide for the current studies, because the alanine-dimer peptide (Ala−Ala) has been well studied as an ideal standard biological peptide. We capped the alanine-dimer peptide with an acethyl group (Ace) at the N terminus and with an N-methyl group (NMe) at the C terminus to eliminate large electrostatic interactions between the termini. The peptide, Ace−Ala−Ala−NMe, was immersed in a cubic box of water with an edge length of 36 Å and solvated with 1541 water molecules for a total of 4655 atoms in the system. We used the Amber96 force field for the peptide and the TIP3P model for water.[29]

Preparation and equilibration procedures for a production run of the system were as follows. The positions of the modeled hydrogen atoms were adjusted by energy minimization *in vacuo*. The peptide was then immersed in a water box, which had been pre-equilibrated under NPT conditions with a constant number of particles, temperature (300 K), and pressure (1 atm) using the Berendsen thermostat and barostat.[30] The atoms of the peptide were kept fixed while the solvent was allowed to equilibrate for 200 ps under NVT conditions at 300 K. After the solvent equilibration, we reduced the restraining force for the atoms of the peptide and simulated all atoms of the system under NPT conditions at 300 K and 1 atm of pressure. The covalent bonds and angles including polar hydrogens were constrained and treated as rigid bodies, thus allowing for a simulation time step of 1 fs. A production run of 10 ns was done under NVT conditions, using a Hoover−Evans thermostat at 300 K.[31]

In the PME method, the parameter α of the PME method was set to 0.35 $Å^{-1}$, and the real space cutoff distance was set to 10 Å for all runs. The mesh size was set to $36 \times 36 \times 36$, thus ensuring a grid density of 1 Å for the system with sufficient accuracy from the Ewald method. Moreover, we employed the atom base cutoff scheme for the long-range interactions in both methods. The radius of the neighbor list is 1 Å larger than the cutoff, and it is updated every five steps with a time step of 1 fs for all simulations. The parameters for the FSw-Wolf method are described in detail in the Results and Discussion section.

To evaluate dipole−dipole interactions in a homogeneous polar molecular system, a cubic water system under periodic boundary conditions with an edge length of 36 Å including 1569 water molecules was prepared in addition to the peptide system. We performed canonical ensemble molecular dynamics simulations of the water system at 300 K, using the PME and FSw-Wolf methods. The dipole−dipole interactions were evaluated using the 1 ns trajectories of the water system.

Multicanonical Molecular Dynamics Simulations. We used the force-biased multicanonical molecular dynamics (FBMcMD) simulation method[24] to evaluate the free energy landscape of the peptide. The FBMcMD algorithm has been described elsewhere,[24,26] so here we briefly summarize it. We generated the FBMcMD ensemble by performing constant-temperature MD at an arbitrarily chosen temperature $T_0 = 1/k_B\beta_0$ with force scaling as

$$\frac{\mathrm{d}\mathbf{p}_i}{\mathrm{d}t} = \nu(E)\mathbf{f}_i \tag{3.1}$$

$$\nu(E) = \frac{\partial \alpha_{\mathrm{mc}}(E)}{\partial E} \tag{3.2}$$

where β_0 is the inverse temperature, k_B is the Boltzmann constant, $\mathbf{p}_i$ and $\mathbf{f}_i$ indicate the momentum and the force of the ith atom, respectively, $\alpha_{\mathrm{mc}}(E)$ is the multicanonical temperature, and $\nu(E)$ represents the force scaling factor. Since the $\nu(E)$ values have not been given *a priori*, they should be determined by the following iterative scheme:

$$\nu^{k+1}(E) = \nu^k(E) + \frac{1}{\beta_0} \frac{\partial \ln P^k(E)}{\partial E} \tag{4}$$

Here, $P^k(E)$ is the probability distribution of potential energy from kth iterative run of the FBMcMD. $\nu(E)$ relates to the density of states $\Omega(E)$ through the following equation:

$$\frac{1}{\Omega(E)} = \mathrm{e}^{-\beta_0 \alpha_{\mathrm{mc}}(E)} \tag{5}$$

Once the $\nu(E)$ has converged, the system can realize a random walk on the potential energy space. We set the temperature for the FBMcMD simulation to 300−700 K so that the peptide can sample various structures at this temperature.

We started FBMcMD simulations from the peptides equilibrated by canonical MD. The same system from the canonical MD was used. We set the reference temperature to 250 K. The FBMcMD simulations for the PME method and that with the modified Wolf method were done in the same manner. We note that only nonbonded electrostatic interactions are different between the two simulations. In both simulations, we then obtained flat energy distributions covering a temperature range from 300 to 700 K. We then executed production runs for each simulation for 2×10^7 steps and stored snapshots every 1 ps. All of the simulations were done using the *myPresto* molecular dynamics computing program.[32]

RESULTS AND DISCUSSION

Accuracy of Energies and Forces. In order to evaluate the accuracy of the FSw-Wolf method, we analyzed the trajectories of the energies and forces for the system from the canonical MD simulations as follows.

A total of 1000 snapshots of the atom coordinates, i.e., one every 1 ps, were extracted from the 1 ns trajectory as simulated using the PME method. Then, for each of these structures, we calculated the electrostatic energy using the FSw-Wolf method with four different α values (0.1, 0.12, 0.16, and 0.2 $Å^{-1}$) and 18 different r_c cutoff distances from 8.0 to 16.5 Å with an interval of 0.5 Å. Thus, the electrostatic energies with 72 different FSw-Wolf method parameters were compared to the corresponding energies from the PME method. The differences between the PME and the FSw-Wolf methods were calculated according to the following criteria:

$$E_{\mathrm{err}}(m) = \frac{|E_{\text{FSw-Wolf}}(m) - E_{\mathrm{PME}}(m)|}{|E_{\mathrm{PME}}(m)|} \tag{6.1}$$

$$\langle E_{\mathrm{err}} \rangle = \frac{1}{M} \sum_{m=1}^{M} E_{\mathrm{err}}(m) \times 100 \tag{6.2}$$

Here, m is the index of each snapshot extracted from the trajectory and M is the total number of snapshots. A comparison of the force vectors of the two methods was made using eq 7:

$$F_{\mathrm{err}}(m) = \frac{1}{N} \sum_{i=1}^{N} \frac{|\mathbf{f}^i_{\text{FSw-Wolf}}(m) - \mathbf{f}^i_{\mathrm{PME}}(m)|}{|\mathbf{f}^i_{\mathrm{PME}}(m)|} \tag{7.1}$$

$$\langle F_{\mathrm{err}} \rangle = \frac{1}{M} \sum_{m=1}^{M} F_{\mathrm{err}}(m) \times 100 \tag{7.2}$$

Here, $\mathbf{f}_{\text{FSw-Wolf}}{}^{i}$ and $\mathbf{f}_{\mathrm{PME}}{}^{i}$ are the electrostatic force vectors acting on each atom using the FSw-Wolf method and the PME method, respectively. $F_{\mathrm{err}}(m)$ is the relative amplitude of the force vector difference at the mth snapshot structure, and $\langle F_{\mathrm{err}} \rangle$ is the average difference over all of the snapshots.

In Figure 1, we show the energy errors between the PME method and the FSw-Wolf method with several α parameters as a function of the cutoff length. We can see from the figure that the energy errors decrease with increasing cutoff length. The error with α = 0.05 $Å^{-1}$ was large in the whole range of cutoff length. In the case where the cutoff length is greater than 12 Å, the error was significantly reduced when α was larger than 0.10 $Å^{-1}$. The error was as small as 0.1% with α = 0.12 $Å^{-1}$ and a cutoff length of 16.5 Å.

For comparison with the other cutoff method, we estimated the error from the reaction field (RF) method, which has been useful in many extensive studies. The dashed line in Figure 1 shows the energy error obtained from the RF method[2] with $\varepsilon = \infty$. The error gradually decreases as the cutoff length increases. When we choose a value greater than 0.15 for the α parameter, the error of the FSw-Wolf method is less than that of the RF method for a wide range of cutoff lengths, in this peptide system.

In Figure 2, we show the force error between the PME method and the FSw-Wolf method with various α values as a function of the cutoff length. Although the force errors decreased with increasing cutoff length, the error ratios were 2 to 10 times larger than the energy error ratios. In Figure 2, the force error was about 4% at a cutoff length of 16.5 Å with α = 0.05 $Å^{-1}$. As α increased, the observed force error decreased, and it was as small as 0.82%, at a cutoff length of 16.5 Å with α = 0.12 $Å^{-1}$.

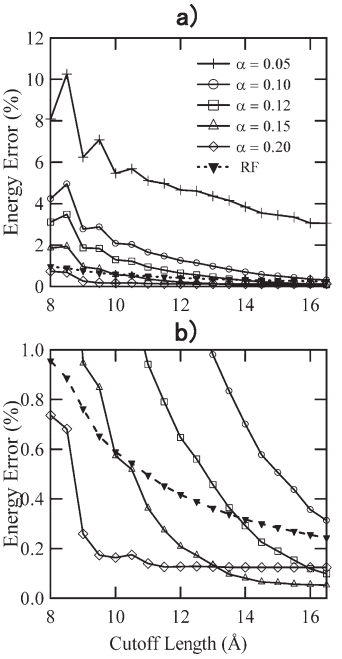

Figure 1. (a) Energy errors of the FSw-Wolf method with various α values from the PME method and the error of the reaction field (RF) method ($\varepsilon = \infty$). (b) Magnified view of the energy error at the small error region.

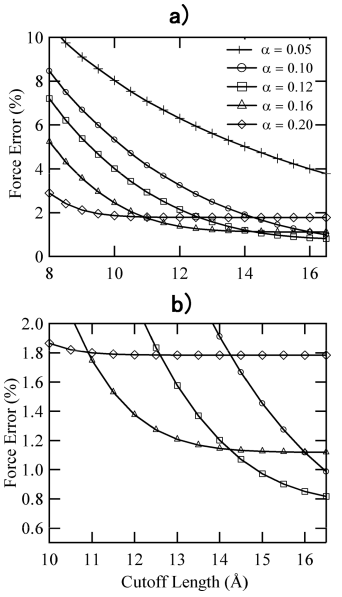

Figure 2. (a) Force errors of the FSw-Wolf method with various α values from the PME method. (b) Magnified view of the force error at the small error region.

The origin of the errors in energies and forces should be due to omission of the reciprocal space contribution of the PME method in the FSw-Wolf method. The reciprocal contributions are reduced by taking a larger cutoff length than the PME method.

As expected, the energy accuracy of the FSw-Wolf method is in good accordance with the PME method. On the basis of results from the canonical MD simulations, respecting the force accuracy, we found that a parameter set consisting of α equal to 0.12 $Å^{-1}$ and a cutoff length of 16.5 Å is optimal for the FSw-Wolf method dealing

Table 1. Timings of the FSw-Wolf (FSWW) and PME Methods with Respect to the Number of CPU in Parallel Computations

	number of CPU				
method	8	16	32	64	128
	single step calculation time (sec)				
PME	0.87	0.61	0.54	0.48	0.51
FSWW (16.5 Å cutoff)	3.57	1.90	1.09	0.66	0.46
FSWW (12.0 Å cutoff)	1.60	0.93	0.59	0.42	0.34

with the peptide system. In addition to the optimal parameter set, we employed another parameter set consisting of α equal to 0.16 $Å^{-1}$ and a cutoff length of 12 Å to examine the features of the smaller cutoff length relative to the optimized parameters. This parameter set yielded 0.2% and 1.37% errors for energy and force, respectively, from those by the PME method. Those parameters were used in the computations hereafter.

Parallel Timings. We investigated the parallel timing in the FSw-Wolf method, because good scalability is generally expected for the simple truncation method. To confirm that the FSw-Wolf method has this advantage, we estimated the timing of the methods for a water system, as a benchmark. We prepared a periodic boundary cubic system including 29 662 pure water molecules with an edge length of 98 Å. For the FSw-Wolf method, cutoff lengths of 16.5 Å and 12 Å were used, with the neighbor list 1 Å larger than the cutoff length. For the PME method, we set a 128 × 128 × 128 fine mesh for the reciprocal space and an 8 Å cutoff for the real space. The calculations were performed on a conventional PC cluster connected by a normal switching-hub with the program *myPresto*, which we previously developed.[32] We used MPI and slab decomposition for FFT parallelization in the PME method. The results are displayed in Table 1.

The table shows that the timing of the FSw-Wolf method with 16.5 Å and that with 12.0 Å cutoffs are faster than the timing of the PME method over 128 CPUs and that over 64 CPUs, respectively. Similar results for PME were also obtained in ref 33, in which a parallel simulation of dihydrofolate reductase, with 23 558 atoms, using a conventional PC cluster with 64 × 64 × 64 mesh and the NAMD program does not show a reduction in the calculation time over about 200 CPUs. Although special machines with optimized networks may show good PME scalability, the FSw-Wolf calculations are faster than the PME calculations with a fine mesh, performed on a conventional PC cluster with normal network connections, even if the system has 88 986 atoms.

The recent technology of the volumetric decomposition has shown to exhibit better scalability than that of the slab decomposition for more than 256 CPUs, when a special high-speed network is applied.[12] On the contrary, when an ordinary simple network is used, the slab decomposition shows good scalability for the smaller number of CPUs than the maximum number of the grid size.

Radial Distribution Function. We have calculated radial distributions between water and the peptide as a function of the radial distance. We calculated the radial distribution of density $g(r)$ using eq 8:

$$g(r) = \frac{\langle N(r)_{\delta r} \rangle}{\frac{4}{3}\pi[(r+\delta r)^3 - r^3]} \tag{8}$$

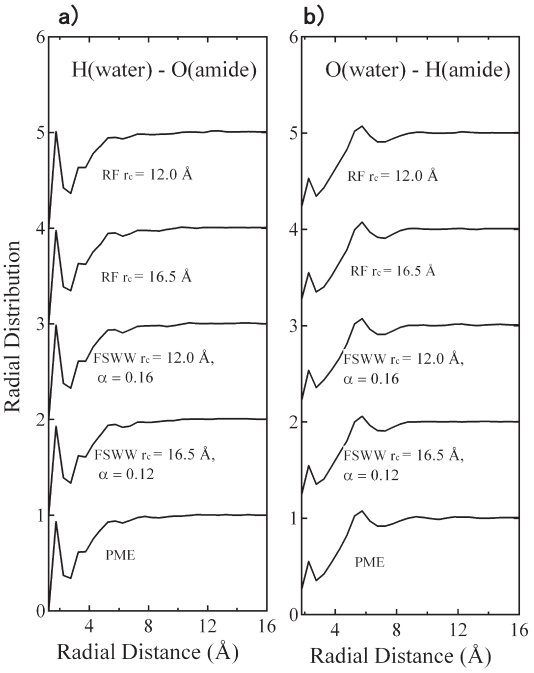

Figure 3. Radial distribution of (a) water hydrogen and peptide oxygen and (b) water oxygen and hydrogen in the peptide bond as a function of radial distance from the PME method and the FSw-Wolf methods (FSWW) and Reaction Field (RF) methods. Except for PME, the base lines are shifted for comparison. The distributions are normalized to unity at the bulk region of solvent.

where $N(r)_{\delta r}$ is the number of atoms of water between r and $r + \delta r$, and the angular brackets denote the ensemble average.

In Figure 3, we show the radial distribution function (RDF) of water oxygen and the amide hydrogen and that of water hydrogen and the peptide oxygen for the three methods: the PME method, the FSw-Wolf method using a cutoff of 16.5 Å with α = 0.12 $Å^{-1}$ and that using a cutoff of 12 Å with α = 0.16 $Å^{-1}$, and RF methods with cutoffs 12.0 and 16.5 Å. All of the results are almost identical, indicating that the FSw-Wolf and RF methods reproduce the RDFs by PME, even if a cutoff value of 12 Å is used.

Dipole−Dipole Interactions. It has been pointed out that the simple truncation method suffers from either sensitivity or an artifact regarding the dielectric properties, especially for the solvent material.[34] To examine whether this disadvantage also appeared in the FSw-Wolf method, we evaluated the distance-dependent Kirkwood factor using both the PME and FSw-Wolf methods, for a cubic system with an edge length of 36 Å, including 1569 water molecules, at 300 K. The distance-dependent Kirkwood factor $G(r)$, as a function of distance r, describes the angular correlation of the molecules, which have permanent dipole moments, as

$$G(r) = \frac{1}{N}\left\langle \sum_i \left(\frac{\mu_i \sum_{j, r_{ij} < r} \mu_j}{|\mu|^2} \right) \right\rangle \tag{9}$$

where r_{ij} is the distance between the ith and jth molecules, N is the number of molecules, and μ_i and μ_j are the dipole moments of the ith and jth molecules, respectively. <...> denotes the time ensemble average. In Figure 4, the distance-dependent Kirkwood

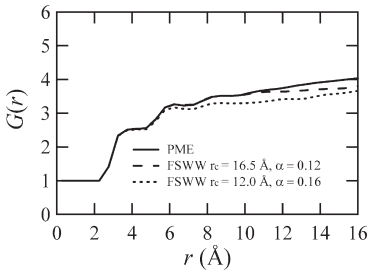

Figure 4. The distance-dependent Kirkwood factor from the PME method (solid line) and the FSw-Wolf (FSWW) methods with r_c = 16.5 Å (dotted line) and 12.0 Å (dashed line).

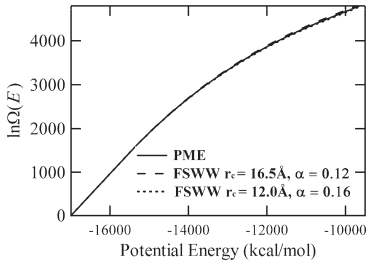

Figure 5. Logarithm of the densities of states $\Omega(E)$ of the peptide system from the PME method and the FSw-Wolf methods (FSWW).

factor, $G(r)$, of the FSw-Wolf method with r_c = 16.5 Å is very similar to that of the PME method, and that with r_c = 12.0 Å is slightly different at the larger distance. The dielectric constants calculated from the distance-independent Kirkwood factor[35,36] are 86.8 (PME), 82.2 (FSw-Wolf method with r_c = 16.5 Å), and 81.1 (FSw-Wolf method with r_c = 12.0 Å). These values are comparable with the results obtained in recent studies,[35,36] although $G(r)$ is very sensitive to the system size and the computation conditions. It is noted that the Kirkwood factor, by means of cutoff methods, is often very different from the PME method, even when much larger cutoff distances are employed.[35] The Kirkwood factors were also reported to deviate with the simple RF method from those with the PME method,[37,38] or to be similar to those with the improved RF method depending on the simulation conditions.[2] Thus, the current FSw-Wolf method with the appropriate parameters should give not only accurate absolute energy values but also reliable dynamic properties.

Free Energy Landscapes of the Alanine-Dimer Peptide. We carried out three different McMD simulations, the first one using the PME method, the second one using the FSw-Wolf methods employing the optimized parameters described above, and the third one employing the shorter cutoff length of 12 Å with α = 0.16 $Å^{-1}$. We obtained flat energy distributions and converged densities of states $\Omega(E)$ for all of the cases. The three densities of state are shown in Figure 5.

In this figure, the three densities of state coincide with each other, indicating that the three systems are thermodynamically very similar.

We have taken the trajectories from the McMD simulations. The length of each trajectory was 20 ns. We then plotted the free energy landscape of the peptide reweighted at 300 K with respect to the distance between the carbon atom of the C-terminal methyl and the carbon atom of the N-terminal methyl in the peptide, as shown in Figure 6.

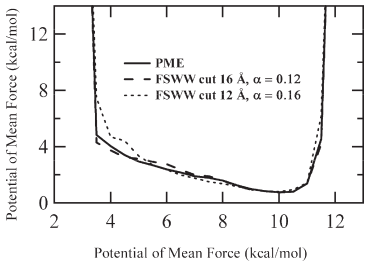

Figure 6. Potentials of mean force at 300 K as a function of the distance between the carbon atom of the C-terminal methyl and the carbon atom of the N-terminal methyl in the peptide from the PME method and the FSw-Wolf methods (FSWW).

From the figure, it is apparent that the peptides are distributed widely from the extended to the twisted conformations. Furthermore, we see that the free energy landscapes from the PME method and from the two FSw-Wolf methods are almost identical. It suggests that the conformational outlines of the peptide obtained from the two methods bear a very close resemblance.

The backbone dihedral angles of the peptide well describe the conformations. So far, there are experimental and theoretical conformational studies of short peptides, and they employed the dihedral angles to evaluate the conformational space.[39,40] To compare the conformational free energy landscapes from both methods, we used the potential of mean force with respect to dihedral angles of the peptide. We employed a pair of the dihedral angles, say, (ϕ_1, ψ_1) and (ϕ_2, ψ_2). Here, ϕ_1 and ψ_1 are first alanine backbone dihedral angles, and ϕ_2 and ψ_2 are the second ones. We show the free energy landscapes of the dihedral angles reweighted to 300 K in Figures 7−9.

In the lower panels of Figures 8 and 9, we depict the absolute free energy difference between the FSw-Wolf method and the PME method. The white regions of the figures indicate that the differences are smaller than 1 kcal/mol. As shown in the figures, the free energy landscapes have a strong resemblance to each other. We see that free energy local minimums, major basins, of C_S^{ext} in the vicinity of ($\phi = -150°$, $\psi = 150°$), P_{II} in ($-70°$, $140°$), and α_R' in ($-60°$, $-60°$) in the PME method are well reproduced in the FSw-Wolf method. On the contrary, slightly different distributions of the free energies in the FSw-Wolf method from the PME methods are found around the shallow basins, the free energies of which are much higher than those of the major basins. However, such differences in the free energy landscapes do not significantly contribute to the conformational distributions.

Consequently, from a comparison between the FSw-Wolf method and the PME in terms of the energies, forces, radial distribution functions, dipole−dipole interactions, and the free energy landscapes of the alanine-dimer peptide in explicit water, it is concluded that the FSw-Wolf method with the optimized parameters or even with the shorter cutoff length of 12 Å with α equal to 0.16 $Å^{-1}$ yields very similar results to the PME method. This fact shows that the criteria regarding the choice of the parameter values with respect to the force error in the FSw-Wolf method surely ensures a good reliability of the method. In addition, we can also get similar results along with the computational efficiency even if we loosen the criteria.

In order to avoid the discontinuity at the cutoff length r_c for the force function originally derived from the Wolf method, we used a switching force function instead of the shifted force approach as proposed in ref 18. Since these two approaches deform the original force function, leading to the deformation of the original

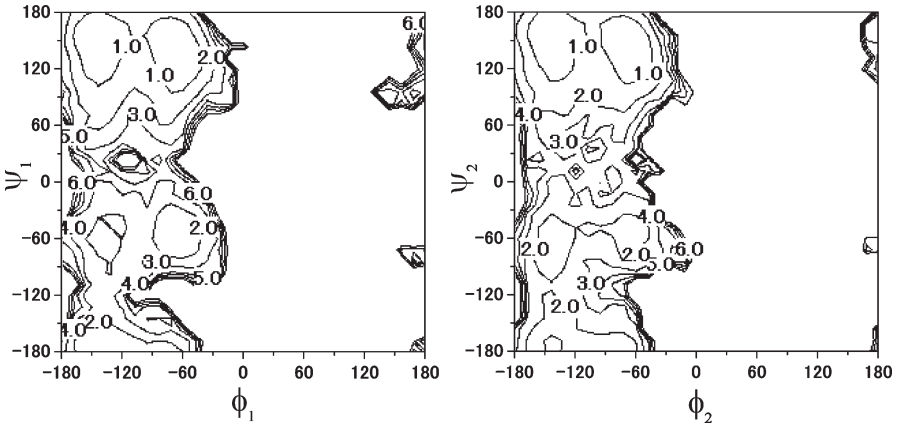

Figure 7. The free energy landscapes of the couples of dihedral angles of the peptide reweighted to 300 K using the PME method. The left-hand side and right-hand side display (ϕ_1, ψ_1) and (ϕ_2, ψ_2), respectively. Units are kcal/mol.

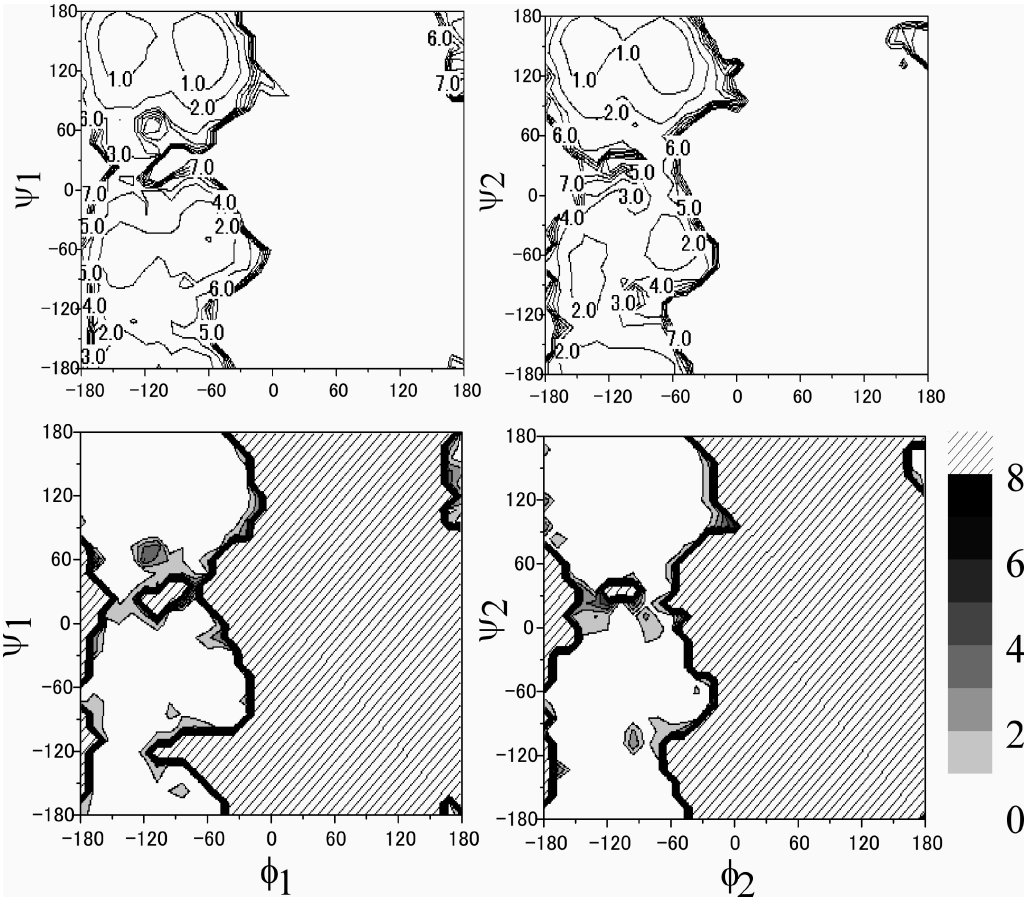

Figure 8. Upper panel: The free energy landscapes of the couples of the dihedral angles of the peptide reweighted to 300 K using the FSw-Wolf method with the optimized parameter set of cutoff length 16.5 Å with $\alpha = 0.12$ Å^{-1}. Lower panel: The absolute value of the free energy difference from the PME method. Left-hand side and right-hand side display (ϕ_1, ψ_1) and (ϕ_2, ψ_2), respectively. The area illustrated by the oblique lines shows a difference larger than 8 kcal/mol. Units are kcal/mol.

potential function, they both need a correction of the total energy. As described in ref 20, this correction can be successfully done in the switching force approach, while it is nontrivial in the shifted force approach. In fact, in the latter, the correction depends on the potential parameters α and r_c, and also on $|r_{ij}| - r_c$, namely, the particle configuration. Thus, it should keep away from a simple correction.[41] In addition, in contrast to the shifted force approach, the current switching force approach can easily induce smoothness of the force function, which is required in the stable numerical integration in MD.[28]

A previous study in ref 20 showed that the electrostatic energy by means of the FSw-Wolf method of a highly charged system,

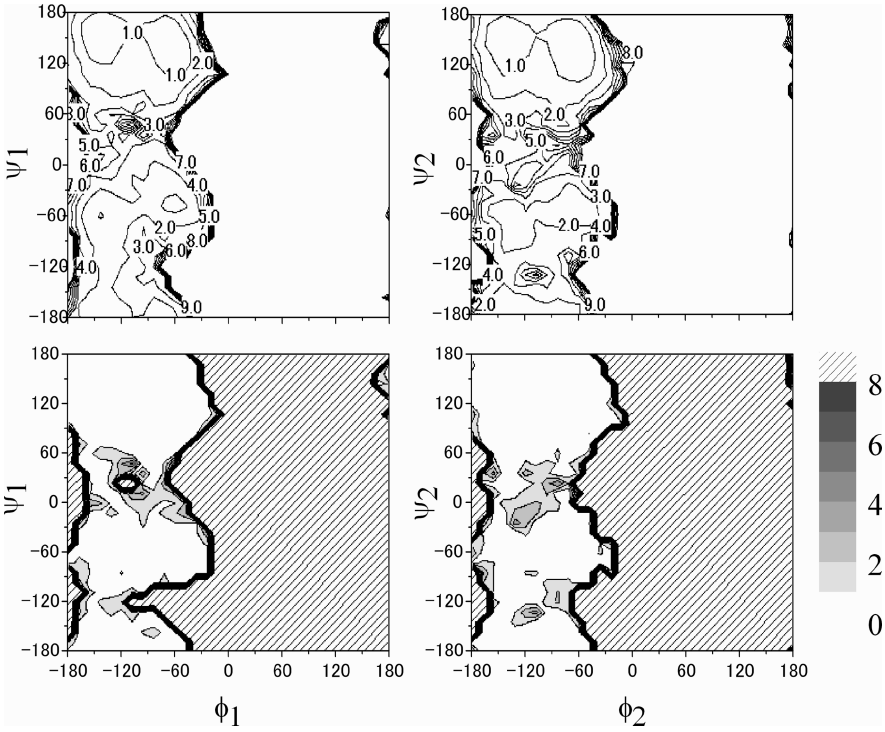

Figure 9. Upper panel: The free energy landscapes of the couples of dihedral angles of the peptide reweighted to 300 K using the FSw-Wolf method with the parameter set of cutoff length 12 Å with $\alpha = 0.16$ Å^{-1}. Lower panel: The absolute value of free energy difference from the PME method. Left-hand side and right-hand side display (ϕ_1, ψ_1) and (ϕ_2, ψ_2), respectively. The area illustrated by the oblique lines shows a difference larger than 8 kcal/mol. Units are kcal/mol.

sodium chloride, was in accordance with that of the Ewald method. High statistical simulation studies on the charged protein system, using the FSw-Wolf method, are in progress.

CONCLUSION

Accurate and rapid computations for electrostatic interactions are of significant importance. Although the Ewald-like method is generally regarded as the standard for calculations of condensed matters' MD and MC simulations under periodic boundary conditions, many alternative methods have been proposed in order to overcome the problem of intrinsic artifacts and the lack of scalability on highly parallel computations. Utility of real space approximations for the Ewald summation is that they are free from the all-to-all networking procedure on the frequency-space calculation, which severely prevents a good scalability with respect to the number of particles, especially in a large system. In this respect, the original Wolf method[13] and the FSw-Wolf method proposed by Fukuda and co-workers[20] as well as other alternatives are expected to be promising alternatives to the Ewald method for treating large systems with highly parallel computations, which have been one of the major trends in computational science, such as in multiscale physics studies. In fact, as demonstrated in one of our previous works,[19] these Wolf type methods have significant advantages, regarding the scalability and the highly parallel calculations on massive PC clusters.

Among the variants of the Wolf method having these advantageous features regarding the computational cost, the FSw-Wolf method presents a consistent MD scheme with a successful energy correction and a sufficient smoothness of the energy function.[20] In this work, we have thus evaluated a physical reliability of the FSw-Wolf MD method in a biological system, using an alanine-dimer peptide in explicit water. Compared with the PME method using the canonical MD simulations, we first determined an optimized set of the parameters for the FSw-Wolf method. The optimized parameters and the other parameters employing a smaller cutoff length of 12 Å yielded comparable energies, forces, and radial distributions to those of the PME method. Then, we carried out force-biased multicanonical molecular dynamics simulations using the two parameter sets to evaluate the free energy landscape of the alanine-dimer peptide with respect to the conformational space. The results at 300 K obtained from the multicanonical molecular dynamics were in accordance with those of the PME method.

By using the canonical MD simulation and the McMD simulation, which is highly reliable, especially in view of the free energy estimation, we consequently show that the FSw-Wolf method is a promising alternative to the PME method with respect to physical accuracy. Advantageous features regarding the computational cost for the Wolf and the variant methods remain in the FSw-Wolf method. Thus, we believe that the FSw-Wolf method should be very useful for simulating large biological systems, in particular, for highly parallel computations.

APPENDIX

We here describe how the total electrostatic energy in the system that contains covalent bond interactions is evaluated in the FSw-Wolf method. The total energy of such a system is represented as

$$E^{\text{total}} = \frac{1}{2}\sum_{i=1}^{N}\sum_{j(\neq i)}^{N}\frac{q_i q_j}{r_{ij}} - \frac{1}{2}\sum_{i=1}^{N}\sum_{j\,\in\, N_{ii}^{\text{CB}}}\frac{q_i q_j}{r_{ij}} \qquad \text{(A1)}$$

where $j \in N_{ii}^{CB}$ means that atoms i and $j(\neq i)$ are submitted to covalent bond interactions, e.g., bond, angle, torsion interactions for "1−2, 1−3, and 1−4 pairs". By using eq 1.1 for the first term in eq A1, we get

$$E^{\text{total}} \sim \frac{1}{2}\sum_{i=1}^{N}\sum_{j(\neq i)}^{N} q_i q_j \tilde{V}(r_{ij}) - \left[\frac{1}{2}\frac{\text{erfc}(\alpha r_1)}{r_1} - \frac{1}{2}V^*(r_1) + \frac{\alpha}{\sqrt{\pi}}\right]\sum_{i=1}^{N} q_i^2 - \frac{1}{2}\sum_{i=1}^{N}\sum_{j \in N_{ii}^{CB}} \frac{q_i q_j}{r_{ij}} \quad \text{(A2)}$$

and thus

$$E^{\text{total}} \sim \frac{1}{2}\sum_{i=1}^{N}\sum_{j \notin N_{ii}^{CB} \cup \{i\}}^{N} q_i q_j \tilde{V}(r_{ij}) - \left[\frac{1}{2}\frac{\text{erfc}(\alpha r_1)}{r_1} - \frac{1}{2}V^*(r_1) + \frac{\alpha}{\sqrt{\pi}}\right]\sum_{i=1}^{N} q_i^2 + \frac{1}{2}\sum_{i=1}^{N}\sum_{j \in N_{ii}^{CB}} q_i q_j \left[\tilde{V}(r_{ij}) - \frac{1}{r_{ij}}\right] \quad \text{(A3)}$$

where $j \notin N_{ii}^{CB} \cup \{i\}$ indicates that atoms i and j are submitted to only nonbonded interactions. It may be convenient for the implementation to use the following deformation in the last term of eq A3, viz.,

$$\tilde{V}(r_{ij}) - \frac{1}{r_{ij}} \sim -\frac{\text{erf}(\alpha r_{ij})}{r_{ij}} - \frac{\text{erfc}(\alpha r_1)}{r_1} + V^*(r_1) \quad \text{(A4)}$$

where we have used eq 1.2 and the assumption that r_1 is sufficiently large, i.e., $r_1 > r_{ij}$ for $j \in N_{ii}^{CB}$. According to eq A4, we have

$$E^{\text{total}} \sim \frac{1}{2}\sum_{i=1}^{N}\sum_{j \notin N_{ii}^{CB} \cup \{i\}}^{N} q_i q_j \tilde{V}(r_{ij}) - \frac{1}{2}\sum_{i=1}^{N}\sum_{j \in N_{ii}^{CB}}^{N} \frac{q_i q_j}{r_{ij}}\text{erf}(\alpha r_{ij}) - \left[\frac{1}{2}\frac{\text{erfc}(\alpha r_1)}{r_1} - \frac{1}{2}V^*(r_1)\right]\left\{\sum_{i=1}^{N} q_i\left(q_i + \sum_{j \in N_{ii}^{CB}}^{N} q_j\right)\right\} - \frac{\alpha}{\sqrt{\pi}}\sum_{i=1}^{N} q_i^2 \quad \text{(A5)}$$

and so the force is

$$\mathbf{f}^{\text{total}\,i} \sim \sum_{j \notin N_{ii}^{CB} \cup \{i\}}^{N} q_i q_j \tilde{F}(r_{ij})\frac{\mathbf{r}_{ij}}{r_{ij}} - \sum_{j \in N_{ii}^{CB}}^{N} \frac{q_i q_j}{{r_{ij}}^2}\left[\frac{2\alpha r_{ij}}{\sqrt{\pi}}e^{-(\alpha r_{ij})^2} - \text{erf}(\alpha r_{ij})\right]\frac{\mathbf{r}_{ij}}{r_{ij}} \quad \text{(A6)}$$

AUTHOR INFORMATION

Corresponding Author

*E-mail: yasuyon33@protein.osaka-u.ac.jp.

ACKNOWLEDGMENT

We thank Dr. Daron M. Standley for the helpful comments and careful reading of the manuscript. This research was supported by Research and Development of the Next-Generation Integrated Simulation of Living Matter, a part of the Development and Use of the Next-Generation Supercomputer Project of the Ministry of Education, Culture, Sports, Science and Technology (MEXT).

REFERENCES

(1) Schreiber, H.; Steinhauser, O. *Biochemistry* **1992**, *31*, 5856–5860.
(2) Schulz, R.; Lindner, B.; Petridis, L.; Smith, J. C. *J. Chem. Theory Comput.* **2009**, *5*, 2798–2808.
(3) Ding, H.; Karasawa, N.; Goddard, W. A., III. *J. Chem. Phys.* **1992**, *97*, 4309.
(4) Board, J. A., Jr.; Causey, J. W.; Leathrum, J. F., Jr.; Windemuth, A.; Schulten, K. *Chem. Phys. Lett.* **1992**, *198*, 89.
(5) Steinbach, P. J.; Brooks, B. R., Jr. *J. Comput. Chem.* **1994**, *15*, 667.
(6) Essmann, U.; Perera, L.; Berkowitz, M. L.; Darden, T.; Lee, H.; Pedersen, L. G. *J. Chem. Phys.* **1995**, *103*, 8577–8593.
(7) Darden, T.; York, D.; Pederson, L. *J. Chem. Phys.* **1993**, *98*, 10089–10092.
(8) Hunenberger, P. H.; McCammon, J. A. *J. Chem. Phys.* **1999**, *110* (4), 1856–1872.
(9) Smith, P. E.; Pettitt, B. M. *J. Chem. Phys.* **1996**, *105* (10), 4289–4293.
(10) Figueirido, F.; Del Buono, G. S.; Levy, M. *J. Chem. Phys.* **1995**, *103* (14), 6133–6142.
(11) Kia, A.; Kim, D.; Darve, E. *J. Comput. Phys.* **2008**, *227*, 8551–8567.
(12) Oh, K. J.; Deng, Y. *Comput. Phys. Commun.* **2007**, *177*, 426–431.
(13) Wolf, D.; Keblinski, P.; Phillpot, S. R.; Eggebrecht, J. *J. Chem. Phys.* **1999**, *110*, 8254.
(14) Demontis, P.; Spanu, S.; Suffritti, G. B. *J. Chem. Phys.* **2001**, *114*, 7980.
(15) Zahn, D.; Schilling, B.; Kast, S. M. *J. Phys. Chem. B* **2002**, *106*, 10725.
(16) Ma, Y.; Garofalini, S. H. *J. Chem. Phys.* **2005**, *122*, 094508.
(17) Avendaño, C.; Gil-Villegas, A. *Mol. Phys.* **2006**, *104* (9), 1475.
(18) Fennell, C. J.; Gezelter, J. D. *J. Chem. Phys.* **2006**, *124*, 234104.
(19) Kikugawa, G.; Apostolov, R.; Kamiya, N.; Taiji, M.; Himeno, R.; Nakamura, H.; Yonezawa, Y. *J. Comput. Chem.* **2009**, *30* (1), 110–8.
(20) Fukuda, I.; Yonezawa, Y.; Nakamura, H. *J. Phys. Soc. Jpn.* **2008**, *77* (11), 114301–114305.
(21) Villarreal, M. A.; Montich, G. G. *J. Biomol. Struct. Dyn.* **2005**, *23*, 135–142.
(22) Hansmann, U. H. E.; Okamoto, Y.; Eisenmenger, F. *Chem. Phys. Lett.* **1996**, *259* (3−4, 6), 321−330.
(23) Nakajima, N.; Nakamura, H.; Kidera, A. *J. Phys.Chem. B* **1997**, *101*, 817–824.
(24) Kim, J. G.; Fukunishi, Y.; Kidera, A.; Nakamura, H. *Phys. Rev. E* **2003**, *68*, 21110.
(25) Nakajima, N.; Higo, J.; Kidera, A.; Nakamura, H. *J. Mol. Biol.* **2000**, *296*, 197–216.
(26) Watanabe, Y.; Kim, J. G.; Fukunishi, Y.; Nakamura, H. *Chem. Phys. Lett.* **2004**, *400*, 258–263.
(27) Kim, J. G.; Fukunishi, Y.; Kidera, A.; Nakamura, H. *Phys. Rev. E* **2004**, *70*, 57103.
(28) Queyroy, S.; Nakamura, H.; Fukuda, I. *J. Comput. Chem.* **2009**, *30*, 1799–1815.
(29) Jorgensen, W. L.; Chandrasekhar, J.; Madura, J. D.; Impey, R. W.; Klein, M. L. *J. Chem. Phys.* **1983**, *79*, 926.
(30) Berendsen, H. J. C.; Postma, J. P. M.; van Gunsteren, W. F.; DiNola, A.; Haak, J. R. *J. Chem. Phys.* **1984**, *81*, 3684.
(31) Hoover, W. G.; Ladd, A. J. C.; Moran, B. *Phys. Rev. Lett.* **1982**, *48*, 1818–1820. Evans, D. J. *J. Chem. Phys.* **1983**, *78*, 3297.
(32) Fukunishi, Y.; Mikami, Y.; Nakamura, H. *J. Phys. Chem. B* **2003**, *107*, 13201.
(33) Bowers, K. J.; Chow, E.; Xu, H.; Dror, R. O.; Eastwood, M. P.; Gregersen, B. A.; Klepeis, J. L.; Kolossváry, I.; Moraes, M. A.; Sacerdoti, F. D.; Salmon, J. K.; Shan, Y.; Shaw, D. E. Proceedings of the ACM/IEEE Conference on Supercomputing (SC06), Tampa, Florida, November 11−17, 2006.

(34) Alper, H. E.; Levy, R. M. *J. Chem. Phys.* **1989**, *91* (2), 1242–1251.
(35) Yonetani, Y. *J. Chem. Phys.* **2006**, *124*, 204501.
(36) Takahashi, K.; Narumi, T.; Yasuoka, K. *J. Chem. Phys.* **2010**, *133*, 014109.
(37) Belhadj, M.; Alper, H. E.; Levy, R. M. *Chem. Phys. Lett.* **1991**, *179*, 13–20.
(38) van der Spoel, D.; van Maaren, P. J. *J. Chem. Theory Compt.* **2006**, *2*, 1–11.
(39) Christoph, F. W.; Weisshaar, J. C. *J. Phys. Chem. B* **2003**, *107*, 3265–3277.
(40) Vargas, R.; Garza, J.; Hay, B. P.; Dixon, D. A. *J. Phys. Chem. A* **2002**, *106*, 3213–3218.
(41) Leach, A. R. *Molecular Modelling: Principles and Applications*, 2nd ed.; Prentice Hall: New York, 2001.